

The prospects for finding brown dwarfs in eclipsing binary systems and measuring brown dwarf properties

D. J. Pinfield¹, H. R. A. Jones¹ and I. A. Steele¹

*Astrophysics Research Institute, Liverpool John Moores University, 12 Quays House,
Egerton Wharf, Birkenhead, CH41 1LD*

dpi@astro.livjm.ac.uk

ABSTRACT

We present the results of a simulation to investigate the prospects of measuring mass, age, radius, metallicity and luminosity data for brown dwarfs in fully eclipsing binary systems around dwarf spectral types from late K to early M that could be identified by ultra-wide-field transit surveys such as SuperWASP. These surveys will monitor approximately a million K and M dwarfs with $|b| > 20^\circ$ (where blending of sources is not a significant problem) at a level sufficient to detect transits of low luminosity companions. We look at the current observational evidence for such systems, and suggest that $\sim 1\%$ of late K and early-mid M dwarfs could have a very close (~ 0.02 AU) BD companion. With this assumption, and using SuperWASP as an example, our simulation predicts that ~ 400 brown dwarfs in fully eclipsing binary systems could be discovered. All of these eclipsing binaries could yield accurate brown dwarf mass and radius measurements from radial velocity and follow-up light curve measurements. By inferring the brown dwarf effective temperature distribution, assuming a uniform age spread and an $\alpha=0.5$ companion brown dwarf mass function, the simulation estimates that brown dwarf brightness could also be measurable (at the 10% level) for ~ 60 of these binary systems from near infrared follow-up light curves of the secondary eclipse. We consider irradiation of these brown dwarfs by their primary stars, and conclude that it would be below the 10% level for $\sim 70\%$ of them. This means that in these cases the measured brown dwarf brightnesses should essentially be the same as those of free-floating counterparts. The predicted age distribution of the primaries is dominated by young systems, and ~ 20 binaries could be younger than 1 Gyr. Irradiation will be below the 10% level for $\sim 80\%$ of these. We suggest that many of these young binary systems will be members of “kinematic moving groups”, allowing their ages to be accurately constrained.

Subject headings: stars: low-mass, brown dwarfs – stars: fundamental parameters – binaries: eclipsing – techniques: photometric

1. Introduction

The mass of a brown dwarf (BD) is arguably its most basic characteristic. The essence of the classification of an object as a BD depends on the objects sustaining deuterium burning (for solar metallicity $>0.013M_{\odot}$) but not sustaining hydrogen burning (for solar metallicity $<0.075M_{\odot}$). However, since BDs contract, cool and fade with time, their observable properties depend strongly on both age and mass. Furthermore, because BD colours are strongly influenced by atmospheric dust formation and molecular absorbers (like H₂O), their appearance will depend not only on effective temperature (T_{eff}) and surface gravity (g), but also on composition. Accurate BD mass, age, radius, metallicity and luminosity data are thus vital to properly test our understanding of these extreme objects.

In view of the particular importance of such data for BDs, it is unfortunate that it has thus far not been possible to completely characterise *any* BDs in this way. There are several reasons for this. In order to measure BD masses, one must find BDs in binary systems, and measure the orbits. One also needs to be able to measure the BD itself to determine its luminosity, and the age of the binary must be established, so as to infer the age of the BD. Proper motion measurements have shown that $\sim 10\%$ of solar type stars have BD companions at wide (>1000 AU) separations (Gizis et al. 2001). However, the periods of such binaries are much too long to be useful in measuring masses. A small number of possible close BD companions to solar type stars have been identified (Halbwachs et al. 2000; Nidever et al. 2002; Blundell et al. 2004). But such systems are very rare, and could not be directly imaged anyway because of the glare of the primary. For the lowest mass stars, adaptive optics imaging has shown that close (~ 1 AU) BD companions to late M and early L dwarfs are significantly more common (Close et al. 2003), with orbits that can be measured in a few years, and binary components that can be individually studied. For example, Bouy et al. (2004) astrometrically measured 36% of the 10 yr orbit of 2MASS 0746+2000AB, constraining the system mass at the 10% level. However, the ages of such binaries will in general be very difficult to constrain without recourse to the theoretical models that one wishes to test. For instance, Bouy et al. compared 2MASS 0746+2000 A and B to Dusty model predictions (Chabrier et al. 2000) in a K, J-K colour-magnitude diagram (CMD) and estimated a system age of 150–500 Myrs. However, when compared to late M and L dwarfs with accurate parallaxes, 2MASS 0746+2000 A and B do not lie above the CMD sequence as sources of this age should. A potentially more useful type of system is represented by the

Epsilon Indi multiple, which consists of a double BD binary (visual separation of 2.65AU) at a distance of 1500AU from its K5 primary (McCaughrean et al. 2004). The BD binary orbit should be measurable ($P \sim 15$ yrs), and the age of the system can be constrained to some degree (0.8-2Gyrs) by measurements of the K dwarf primary (Lachaume et al. 1999). However, such multiple systems are not common place, and age constraints established from measurements of a single primary star will not generally be very precise.

The concept presented here is to exploit the new breed of ultra-wide-field transit surveys (designed primarily to find signatures of planetary transits) to identify BDs in fully eclipsing close binary systems around cool stars. BD masses could be measured from the doppler wobble of the primary (using radial velocity techniques). One could measure BD radii from the depth of the primary eclipse (when the BD crosses the face of the primary). The brightness of the BD may be measured from the secondary eclipse (when the BD goes behind the primary) provided the BD is bright enough compared to the primary. Many of these systems will be young (because BDs are brighter when young), making membership of young kinematic moving groups more likely. Membership of such moving groups would accurately constrain age and metallicity.

In this paper, we discuss the prospects of identifying BDs in binaries capable of providing the full compliment of BD mass, age, radius, metallicity and luminosity data. In Section 2 we discuss what is currently known about the frequency and separation of close BD companions, and how this effects the likelihood of eclipse. In Section 3 we use the SuperWASP survey as an example of the new ultra-wide-field transit surveys, estimate sensitivities and the effects of source crowding in images with very large pixels, and estimate the distances out to which BD transits should be detectable. Section 4 describes the additional factors limiting the number of suitable binary systems; the accuracy with which secondary eclipses can be measured (Section 4.1), and the limits imposed by the doppler wobble technique (Section 4.2). Section 5 gives some background on kinematic moving groups, and details how one could accurately constrain the ages of young systems. Section 6 describes our simulation to predict the size and properties of the eclipsing BD population. Section 7 then discusses some identification and followup procedures, and Section 8 presents our conclusions.

2. Close BD companions

2.1. Frequency and separation

In Table 1 we show and compare what is known about the frequency of companion stars and BDs as a function of separation. For solar type stars, Halbwachs et al. (2003)

and Duquennoy & Mayor (1991) have measured the frequency of stellar companions as a function of period (which we convert into separation), using 10 years of radial velocity data combined with visual binaries and common proper motion systems. It is clear from this work that stellar companions are common over a large range of separation. However, it has been known for some time that there is a dearth of low mass ratio ($q \leq 0.1$) companions in close orbits around solar type stars, known as the “BD desert”. Other radial velocity surveys (eg. Marcy & Benitz 1989; Fischer & Marcy 1992; Nidever et al. 2002) have now studied large numbers of solar type stars, and it is currently estimated that $\leq 1/500$ have a BD companion within 3AU (Vogt et al. 2002). This corresponds to a BD companion fraction of $< 0.07\%$ per decade in separation (clearly much less than the $\sim 4\%$ for stellar companions. The desert does not extend to wide separations, with sub-stellar companions imaged at 15–20AU (Els et al. 2001; Lui et al. 2002), and BDs are as common in very wide binaries (~ 1000 AU or more) as stellar companions around solar type stars.

In terms of primary type, there is evidence (from the OGLE transit survey) that the desert extends out to the mid-K dwarfs, since the majority of the small low luminosity companions discovered by Udalski et al. (2002a, b, 2003) turned out to be low-mass stars and not BDs (Dreizler et al. 2002). However, for later dwarfs, the target lists for radial velocity surveys are not large enough to accurately constrain the close BD companion fraction. Despite these limitations some interesting candidate BD companions have been discovered. Reid & Mahoney (2000) found a possible BD companion ($0.07\text{--}0.095 M_{\odot}$) at a separation of $\sim 0.005\text{--}0.007$ AU from an $\sim M5$ dwarf in a radial velocity survey of ~ 50 Hyades M dwarfs. Nidever et al. (2002) found 2 possible BD companions (at separations of ~ 0.2 and ~ 2 AU) around early M dwarfs from a radial velocity survey including ~ 100 M dwarfs. Conversely, Marchal (2003) found no close BD companions in a comparable radial velocity survey of ~ 100 M0-5 dwarfs.

At somewhat larger separations, Oppenheimer et al. (2001) found 1 BD in a corona-graphic survey of the stellar population within 8 parsecs of the Sun. This volume limited sample (ie. mostly M dwarfs) consisted of 163 stars in 111 star systems, and BDs with mass $\geq 0.04 M_{\odot}$ and age ≤ 5 Gyrs could have been detected with separations of 40–120AU around 80% of the sample. BDs are not found in significantly wider orbits around early M dwarfs, perhaps because impulsive perturbations by close stellar encounters will cause such weakly bound systems to dissolve (see Burgasser et al. 2003). It is not, then, surprising that this lack of wide BD companions is also seen around the latest stars and BDs (with the possible exception of one very young candidate BD binary which would have a separation of ~ 240 AU; Luhman 2004). However, closer companions to late M, L and T dwarfs are quite common (see Table 2), and while accurate masses are generally not available, many of these will be sub-stellar (eg. Freed et al. 2003; an L7.5 BD ~ 3 AU from an M8 star).

Of interest here are the late K–mid M dwarf primaries, since we will subsequently show that sufficient numbers of these dwarfs will be monitored by ultra-wide-field surveys to find eclipsing BD companions (see Section 6). It is clear from Table 1 that BD companions to these stars could occur at the $\sim 2\%$ level in orbits close enough to make transits likely ($\leq 0.02\text{AU}$; see Section 2.2). However, an accurate determination of the masses of the BD candidates discovered so far would require knowledge of orbital inclination. Some may turn out to be low-mass stars at low inclination (eg. Halbwachs et al. 2000). If correct though, it would show that although the BD companion fraction in close orbits around such stars is lower than that of stellar companions, there would be no BD desert for these primaries.

In addition to these systematic searches, there have been two serendipitous discoveries of possible close BD companions. Schuh et al. (2003) reported the discovery of an eclipsing BD companion to a late K dwarf with a separation of 0.02AU . This system was discovered while photometrically monitoring a white dwarf. Also Santos et al. (2002) discovered a radial velocity BD companion to an M2 dwarf with a separation of 0.017AU . This system was found as a result of the weak gravitational wobble it induced in the visual K2 companion of the M dwarf.

Having considered all known candidates, it can be seen that the spectral type range of the primaries in systems that could potentially harbour significant populations of very close BD companions ranges from late K to mid M. The orbital periods of these BD companions in close orbits around late K–mid M dwarfs is 1–1.5 days. At these separations, a full transit lasts $\sim 1.5\text{hrs}$.

2.2. Eclipsing fraction

The majority of the known candidate BD companions around K and M dwarfs (three out of five) are in close orbits with separations $\leq 0.02\text{AU}$ (see previous section). Close systems such as these will be the most likely to eclipse, because eclipsing probability is $\propto 1/a$ (where a is separation). We therefore chose to consider the likelihood of an eclipse for a BD companion at a separation of 0.02AU . This separation corresponds to $\sim 10R_\star$ for an early M dwarf, and for such separations, a favourable ~ 1 in 15 should be eclipsing. The requirement for a full eclipse is that

$$\sin(90 - i) \leq \frac{R_p - R_{BD}}{a}, \quad (1)$$

where i is the inclination angle, R_p and R_{BD} are the primary and BD radii respectively, and a the component separation. The fraction of sources that should be eclipsing is $(90 - i)/90$. Using theoretical stellar radii from the 500Myr NextGen models of Baraffe et al. (1998), and

assuming $0.1R_{\odot}$ for the BDs (typical for 500Myr age), we get the eclipse fractions shown in Figure 1. As the primary radius decreases, the chances of a full eclipse fall off, and for comparable radii full eclipses are very unlikely. It can be seen that for late K–early M dwarfs, the eclipsing fraction is $\sim 4\text{--}7\%$, and so even with a $\sim 1\%$ binary fraction at 0.02AU, one could still expect to find fully eclipsing BD companions around ~ 1 in 2000 dwarfs of this type.

2.3. Irradiation

Since we are interested in measuring companion BD properties that would be essentially the same as those of free-floating counterparts, we desire irradiation effects to be low. However, for the very close BD companions discussed in Section 2.2, this may not always be the case, since the cool BD companion could be heated by the nearby brighter hotter primary, as happens with giant planets in close orbits around solar type stars (hot Jupiters). Hot Jupiters are strongly irradiated, and have higher T_{effs} and swollen radii as a result (eg. Burrows Sudarsky & Hubbard 2003; Chabrier et al. 2004). Irradiation should only be an issue when the incident flux from the primary is significant compared to the emergent flux from the companion. If the incident flux is 10% of the emergent flux for instance, then the BD luminosity would increase by no more than 10% (and the radius and T_{eff} by much less than this). This level represents a useful level of accuracy with which to measure BD brightness. Figure 2 shows how the amount of irradiation varies for BD companions (spectral types M6-T4) at 0.02AU separation from their primary stars. Each point in the plotting area represents a binary where the primary and secondary spectral types can be read off the y and x axis respectively. Using NextGen model data for the primaries, BD T_{effs} appropriate to their spectral type (Reid et al. 1999; Knapp 2004) and assumed BD radii of $0.1R_{\odot}$, we derived a locus of binary systems in which the BD will be irradiated by 10% of its emergent flux. This locus is plotted in the figure as a solid line, where binaries above the line are not significantly irradiated. For example, an M8 BD will not be significantly irradiated at 0.02AU from a mid K dwarf (or later) primary, and an L4 BD will not be significantly irradiated at 0.02AU from an M0-2 (or later) primary.

2.4. Age and mass distributions

The mass and age distribution of the companion BDs is important because the older and lower mass BDs will be more difficult to measure from the secondary eclipse. The age distribution should be the same as the local disk. An analysis of chromospheric activity of G and M dwarfs in the solar vicinity (Soderblom, Duncan & Johnson 1991; Henry, Soderblom &

Donahue 1996) is consistent with a uniform star formation rate over the age of the disk, and we thus assume that BDs will have a uniform age distribution between 0 and 10Gyrs. The mass distribution of companion BDs is less constrained. The BD mass function slope for the field and young clusters/associations ranges from $\alpha \sim 0.5\text{--}1$ (where $dn/dm \propto m^{-\alpha}$). However, the masses of BDs in close binaries may have a very different distribution, since dynamical factors during formation (eg. Reipurth & Clarke 2001) and possible radial migration (due to early disk interaction; Armitage and Bonnell 2002) could be important. For very low-mass binary systems for instance, the q distribution peaks at 0.7 – 1 (Burgasser et al. 2003; Pinfield et al. 2003). Such a bias amongst binaries with an early M dwarf primary would produce a strong preference for stellar companions over BDs, and the BD companion mass function itself would prefer high mass BDs. However, it is not currently possible to estimate α for close BD companions from the limited observational evidence, and it essentially remains a free parameter. Low values of α would result in proportionally more high mass BDs (for some value of the BD companion fraction), which would be brighter and easier to detect. Higher values would mean proportionally more low-mass BDs, many of which would be too faint to detect.

3. Ultra-wide-field transit surveys

The discovery of the first transiting extra-solar planet (Charbonneau et al. 2000; Henry et al. 2000) has led to a proliferation of ground based photometric searches aiming to detect planets around bright solar type stars by searching for transit signatures in photometric light curves (see Horne 2003). These searches fall into two categories; the deeper, but relatively small area searches such as the Optical Gravitational Lensing Experiment (which uses a 1.3m aperture telescope), and the ultra-wide-field surveys such as SuperWASP (Christian et al. 2004), TrES (Alonso et al. 2004), Vulcan South (Caldwell et al. 2003) and others, that use small aperture (~ 10 cm) wide-field ($5\text{--}10^\circ$) CCD based systems with spatial resolution of $\sim 10'' \text{ pixel}^{-1}$. While accurate light curve extraction is more challenging for ultra-wide-field data, the ultra-wide-field surveys promise to discover transits around brighter nearer stars, for which close transiting companions can be more accurately measured. In this paper we focus on the abilities of these ultra-wide-field surveys, and use the UK's SuperWASP project as a specific example.

3.1. SuperWASP

SuperWASP (Super Wide Angle Search for Planets) is a project to construct and operate facilities to carry out ultra-wide-field unfiltered photometric monitoring surveys (see Pollacco et al, www.superwasp.org). The first SuperWASP facility (SuperWASP-I) is located on Roque de Los Muchachos, La Palma, and a second facility has also been funded for the southern hemisphere. SuperWASP-I consists of five camera units mounted on a large computer controlled fork mounting, housed in a small enclosure. Each camera unit consists of a 200mm f1.8 Canon lens with an aperture of 11.1cm (made of fluorite and UD glass components) and a 2048x2048 pixel e2v42 thinned CCD (BV coated) cooled to -60C by a 3-stage Peltier. Each camera has an 8°x8° field of view, resulting in large 14.3 arcsecond CCD pixels. The combined sky coverage of the five cameras is thus \sim 320 sq. degs. SuperWASP-I current observing strategy is to repeatedly measure 30s integration images of the same region of sky throughout each night for a period of \sim 2 months, before moving onto a new region. With low overheads (\sim 4s readout), SuperWASP-I takes \sim 100 sets of images per hour. First light was in November 2003, and at time of writing SuperWASP-I is routinely taking data. A data reduction pipeline is being implemented, and light curves of all stars measured will be placed on the public “Ledas database” at The University of Leicester, where software search algorithms will be available for data mining.

3.2. SuperWASP sensitivities

SuperWASP is an unfiltered system, and as such the transmission profile (or pass band) is determined by the atmosphere, the optical throughput of the lenses and CCD entrance window, and the CCD quantum efficiency. To estimate the shape of the SuperWASP transmission profile we have used available site and technical details. We used La Palma atmospheric extinctions from the “INT Wide Field Survey” web-site (based on observations by Derek Jones in August 1993). For the Canon lenses, the optical transmission of UD glass and fluorite (\sim 95% per pair of air-glass interfaces) does not vary significantly from \sim 0.23-7 microns (minimising chromospheric aberration). We thus assumed a wavelength independent optical transmission of 75% to allow for the lens groups (in each Canon lens) and the CCD entrance window. The CCD quantum efficiency was taken from the E2V CCD selection guide, interpolating between the -20°C and -100°C curves. Figure 3 shows the atmospheric, lens and CCD transmission profiles (dotted lines) against wavelength, and the resulting total SuperWASP transmission (solid line). The transmission profile peaks in the V and R bands (at \sim 60%). Blue of V, both atmospheric extinction and the CCD quantum efficiency reduce throughput. Red of R the transmission is predominantly reduced by CCD quantum

efficiency. We estimated a system zero point using a spectrum of Vega (from Hayes, 1985 and Mountain et al., 1985), which we take to represent a zero magnitude source. Accounting for the collecting area (96.7 sq. cm for each lens) and the SuperWASP transmission, we integrated the detected Vega photons across the SuperWASP band. The predicted zero point was found to be 21 magnitudes (2.5×10^8 detected counts/s from a zero magnitude source). As a guide, this means that a signal-to-noise of ~ 50 would result from a 30s integration on a 16th magnitude source.

3.3. Unfiltered colour term

We used the spectra of Pickles (1985; available on CDS) and Leggett et al. (2000; from www.jach.hawaii.edu/~skl), combined with a Johnson V-band (Bessell 1990) and the SuperWASP pass band, to derived synthetic V-band and SuperWASP-band flux ratios for early G-mid M dwarfs. These flux ratios were converted into SuperWASP colours ($V - m_{SW}$, where m_{SW} is a magnitude on the natural SuperWASP system) using our Vega spectrum to define zero colour. Figure 4 shows the resulting colour terms as a function of spectral type. It can be seen that for early G dwarfs the colour term is small, but for later spectral types it becomes significant because most of the optical flux from these dwarfs is not in the V-band, but is in the red part of the SuperWASP band.

3.4. Unfiltered sky brightness

To estimate the La Palma sky brightness as seen by SuperWASP, we used the full range of optical sky brightness measurements from Benn & Ellison (1998), for bright, grey and dark sky conditions. For each sky we converted the magnitudes into fluxes using our Vega spectrum (see Section 3.1). The resulting flux levels were then joined together to provide an approximate sky spectrum. These sky spectra were then multiplied through by the SuperWASP band pass, and converted into SuperWASP magnitudes using our system zero point. The SuperWASP sky brightness estimates were found to be 18.3, 20.3 and 21.1 magnitudes per square arcsecond for bright, grey and dark skies respectively. If one accounts for the large SuperWASP pixels and a spatial resolution element containing 12 pixels (a 2 pixel radius aperture), one would expect sky brightnesses of 9.8, 11.8 and 12.6 magnitudes per resolution element, for bright, grey and dark skies respectively.

3.5. Source crowding with large pixels

The large SuperWASP pixels (and consequent large aperture sizes used for photometry) mean that image crowding will be much more of an issue than it is for higher spatial resolution imaging, particularly in the Galactic plane. This is important for two reasons. Firstly, if a transit source shares its aperture with another star (ie. if it is blended), the SNR of the transit detection will be decreased. However, more importantly, if the PSF of a neighbouring source spills into the aperture of a star, this fraction of the measured flux could vary over time if the PSF changes slightly, or the chosen aperture does not remain perfectly centred on the star – SuperWASP tracking (~ 0.01 arcsecond/s accuracy) will cause stars to drift between pixels over several hours. Since we are interested in identifying eclipse dips that are $\sim 4\%$ deep, we would not want such flux pollution much above the 1% level. We have therefore used synthetic gaussian point-spread-functions to determined the distance at which a source (with $FWHM=1.5$ pixels) will pollute it's neighbours 2 pixel aperture by 1%, and established how this distance ($d_{1\%}$) depends on the relative brightness of the two sources (Δmag). We found that

$$d_{1\%} = FWHM \times (1.95 - 0.12\Delta mag), \quad (2)$$

for $\Delta mag < 2.0$. For fainter neighbours, $d_{1\%}$ drops more rapidly, reaching zero for $\Delta mag = 5$ (ie. a factor of 100). So if a source has a neighbour with $d < d_{1\%}$, we consider it significantly blended, and not measured with sufficient accuracy for our purposes by SuperWASP. We applied this criteria to a series of 1 sq. deg catalogues (centred on different Galactic coordinates) from the SuperCOSMOS Sky Survey database¹. Since we are interested in late K and early M dwarfs, we only considered SuperCOSMOS sources with $B_J-R \geq 1.8$, and estimated the fraction of blends as a function of Galactic coordinate and source brightness. We found that for $V \sim 16$, $\sim 30\%$ of sources with $|b| > 20^\circ$, and $\sim 75\%$ of sources with $|b| < 20^\circ$ will be blended in SuperWASP images. For $V \sim 18$, we found 50% and 85% blended fractions for $|b| >$ and $|b| < 20^\circ$ respectively.

3.6. Transit detection magnitude limits

The signal-to-noise level of a transit detection is

$$SNR = \left(\frac{R_{BD}}{R_\star} \right)^2 \left(\frac{S_{\text{obs}}}{\text{noise}_{\text{obs}}} \right) \sqrt{\frac{PR_\star}{t_{\text{obs}} \pi a}}, \quad (3)$$

¹<http://www-wfau.roe.ac.uk/ssss/>

where R_{BD} and R_{\star} are the radii of the companion BD and the primary star, S_{obs} and $\text{noise}_{\text{obs}}$ are the signal detected from the source and the associated noise during an observation, P is orbital period, t_{obs} is the time taken for an observation (~ 30 s), and a is the separation of the binary. The first term represents the relative decrease in brightness during transit, the second term is the signal-to-noise associated with each observation, and the last term is the square root of the number of observations made during a transit. The noise model we used was

$$\text{noise}_{\text{obs}} = \sqrt{(S_{\text{obs}}t_{\text{obs}}) + (S_{\text{sky}}t_{\text{obs}}) + (Dt_{\text{obs}}) + (NR^2) + (\text{Syst}^2)}, \quad (4)$$

where S_{sky} is the signal detected from the sky in an $N=12$ (2 pixel radius) spatial resolution element (cf. the lenses produce a ~ 1.5 pixel point-spread-function) during an observation, D is the dark current ($\sim 0.01e^-/\text{s}$), R is the read-noise ($\sim 12e^-$), and Syst represents any systematic errors. In general, systematic uncertainties associated with relative photometry of bright sources can be reduced to the 1–2 m-mag level (Kane et al. 2004; Bakos et al. 2004). For the fainter sources, of interest here, systematics will be dominated by field crowding effects which sets the upper level of the systematic uncertainties at a self imposed 10 m-mags (see Section 3.4).

We define our transit detection limits requiring a $\text{SNR} \geq 5$. We would only expect 1 in ~ 2 million stars to register a 5σ transit due to random noise alone, and since SuperWASP will survey rather less than this number of late K and M dwarfs, false positives from random noise will not be a problem. We combined equations 2 and 3 with the SuperWASP zero point, and used the binary characteristics and stellar model data described in Section 2.2 to derive SuperWASP magnitude limits for 5σ transit detection. These limits, for bright, grey and dark skies are shown in Figure 5 (solid lines), as a function of primary M_V . Primary spectral types are also indicated at their appropriate position (taken from Pickles 1985). V-band magnitude limits were then derived using the colour term from Section 3.2 (dashed lines). For comparison, the G star 10σ bright sky detection limit of Horne (2003) is over-plotted (open circle), and joined to its 5σ equivalent (filled circle). It is clear from the figure that as one moves to later type stars, transits can be detected out to fainter magnitudes. This is because later stars are smaller, and eclipse dips are correspondingly deeper. Also, the effect of the broad unfiltered pass band is clear, since SuperWASP will do better for red sources than a comparable V-band filtered system.

3.7. Distance limits for transit detections

The V-band transit detection limits from Figure 5 were converted directly into distance limits using the appropriate values of M_V . These distance limits are shown in Figure 6 (solid

lines) for bright, grey and dark skies. It can be seen that transits of late K-early M dwarfs should be detectable out to \sim 200-500pc. For the later mid M dwarfs, SuperWASP is limited to \sim 100pc, due to their fainter intrinsic brightness. The figure also contains some additional limits, which will be described in the next section.

4. Limits imposed by follow up requirements

4.1. Measuring BD brightness from secondary eclipses

Having identified a good transit signature of a low luminosity fully eclipsing companion (and confirmed it with an intermediate sized optical telescope), one can then attempt to measure the brightness of the companion from the secondary eclipse. Our ability to do this is governed by the accuracy with which we can measure follow up light curves and the relative brightness of the companion and primary. Compared to late K/early M dwarfs, BDs with spectral types $< T2$ are relatively brightest in the K-band (see Leggett et al. 2002). K is generally thus the best band in which to search for a secondary eclipse. With $M_V=8-12$ and $M_K=5-7$ (see Reid & Cruz 2002), a typical late K/early M dwarf near the SuperWASP distance limits (500-200pc respectively) would have $K \simeq 13.5$. The accuracy of K-band light curves will depend on photon noise, stability of the instrumental response, and atmospheric conditions. Using 2-4m class telescopes, a signal-to-photon-noise ratio of ~ 1000 could be achievable for a $K \sim 13.5$ source in $\sim 5-10$ minutes. Variations in the zero point and extinction can be corrected for using frequent standard measurements, flat-fielding should be good to at least 0.1% accuracy, and atmospheric scintillation noise for such observations will be ~ 1 part in 10^4 (equation 10 of Dravins et al. 1998). The main source of systematic uncertainty in near infrared photometry is the amount of atmospheric H_2O absorption, which can be variable on very short timescales. Kidger & Martín-Luis (2003) measured high precision near infrared photometry of bright ($K \leq 10$) northern hemisphere stars using a photometer, and were able to obtain K-band accuracies (inferred from multiple measurements) as good as 0.4m-mags for some sources (see their Figure 8). Typical uncertainties would not always be this good, as atmospheric conditions change (cf. Kidger & Martín-Luis' median uncertainty was ~ 3 m-mags), however an overall K-band measurement accuracy of 1m-mag should be a realistic level to aim for. Note that large scale NIR arrays (such as WFCAM on the UK IR Telescope) would allow comparison stars to be measured at the same time as targets, which could reduce atmospheric systematics. However, we will continue to use Kidger & Martín-Luis as our main example, since they have observationally established these levels of accuracy.

The total accuracy with which we can measure the depth of a secondary eclipse dip in a

near infrared light curve (σ_{tot}) will depend on both the accuracy of an individual observation (σ_{obs}) and on the number of data points (N) measured during secondary eclipse (where $\sigma_{tot} = \sigma_{obs} \sqrt{N}$; see Henry et al. 2000). For the binaries we are considering, we would expect an eclipse to last ~ 1.5 hrs, and we could thus expect to obtain 6-10 K-band measurements per eclipse (allowing for 5 minutes overhead per observation). By measuring 3-4 eclipses, and phasing the data appropriately, one could then measure the depth of the secondary eclipse dip with an accuracy of 0.2m-mags. Thus, for an eclipse dip to be measured with 10% accuracy, it must be at least 2m-mags deep. The BD must therefore be no less than 500 times (6.75 mags) fainter than the primary star. Estimating primary M_K from Reid & Cruz (2002), and BD M_K (appropriate for M6-T4 spectral types) from Dahn et al. (2002) and Knapp et al. (2004), we have derived M_V brightness limits for primaries with M_K 6.75 magnitudes brighter than BD companions of each spectral type. These primary M_V limits are shown in Figure 6, where each is labelled with its appropriate BD spectral type. As an example, it should be possible to measure the secondary eclipse of an L6 eclipsing BD companion of an $M_V \geq 9$ primary.

4.2. Measuring BD masses from radial velocities

If a low luminosity eclipsing companion is detectable from its secondary eclipse, then radial velocity techniques can be employed to accurately measure its mass. For eclipsing systems, the inclination is known to better than 1° , and the relative mass of the BD (compared to that of the primary) can be determined by measuring a radial velocity curve for the primary. Primary masses will thus act as anchors for the BD masses, and uncertainties in the mass-luminosity relation for low-mass stars (cf. Henry & McCarthy 1993) will propagate through to the BD masses. However, it is expected that the low-mass star mass-luminosity relation should improve significantly in the next few years, as the orbits of many more M dwarf systems are measured (eg. by the RECONS; Jao et al. 2003).

The radial velocity accuracy required to determine BD masses places its own limits on the distance of useful binary systems. To illustrate this, a $0.05M_\odot$ brown dwarf at 0.02AU will cause a radial velocity oscillation of $\pm 20 \text{ km s}^{-1}$ for a $0.5M_\odot$ M dwarf primary. Standard arc lamp echelle spectroscopy is limited by several factors; zero point drifts in the wavelength scale between exposures, the spectral features available for cross correlation techniques, the presence of telluric absorption, the signal-to-noise of the spectra themselves, and intrinsic properties of the star (surface spots and/or rotation). We will return to the issue of spots and rotation in Section 7.3. For the other factors however, we will use previous optical studies with 8m telescopes as a guide. Reid & Mahoney (2000) observed zero point drifts

of $\pm 1\text{km}\text{s}^{-1}$ during a full night for the Keck HIRES echelle spectrograph. However, they managed to obtain $\pm 300\text{ms}^{-1}$ accuracy by cross correlating echelle orders (containing strong telluric signatures), with white dwarf spectra (which act essentially as continuum sources onto which a clear telluric signature is imprinted). More recently, Konacki et al. (2003) used an iodine cell to more rapidly measure zero point drifts of $\sim 200\text{ms}^{-1}$ over timescales of ~ 30 minutes. These studies looked mostly at K and M dwarfs from 3850–6200Å and 6350–8730Å respectively, and found that such drifts generally dominate the overall uncertainty, with contributions of only $\pm 60\text{ms}^{-1}$ coming from the signal-to-noise (~ 15 –25) of the spectra themselves.

It is thus clear that optical echelle spectroscopy should be capable of providing radial velocities with accuracies of $\pm 0.5\text{km}\text{s}^{-1}$ (enough to constrain close BD companion masses at the ~ 2 –3% level) using lower signal-to-noise spectra from rather fainter sources with $V \sim 19$. We have converted this magnitude limit into a distance limit which is shown in Figure 6 (dashed line). It can be seen that for sources with spectral types $< M4$ the echelle followup requirements do not impose any additional distance constraints beyond those of SuperWASP itself. The efficient follow up of later type primaries at the SuperWASP distance limit would require a near infrared echelle spectrograph (such as PHOENIX on Gemini). However, we do not expect to find many of these as fully eclipsing systems (see Sections 2.2 and 6).

5. Determining accurate ages

5.1. Open clusters

Disk stars with the best constrained ages are those in open clusters. The age of an open cluster can be well constrained using a variety of methods, such as fitting the upper main sequence turn off (Sarajedini et al. 1999), or (for young clusters) measuring the magnitude of the lithium depletion edge (Stauffer, Schultz & Kirkpatrick 1998). An open cluster is believed to be a coeval association (with only a relatively small age spread of perhaps a few Myrs). Therefore, if membership of a cluster is established, then the cluster age can be assumed for the star. However, the majority of disk stars are not open cluster members. Within the SuperWASP distance limits ($\sim 500\text{pc}$) there are ~ 31 open clusters in the La Palma sky (see the LEDAS database²). Although catalogued membership of these clusters is by no means complete, a reasonable estimate would be that between them they contain no more than a few thousand late K/early M dwarfs. This represents a tiny fraction of the number of non

²<http://ledas-www.star.le.ac.uk>

cluster disk stars of this type in the SuperWASP sky (~ 1 million). Open cluster membership will thus not be very useful for constraining the age of a significant fraction of the binary systems under consideration.

5.2. Young moving groups

Open clusters are thought to represent only small components of larger kinematically distinct coeval populations that are spatially dispersed within the disk. Such disk populations are known as moving groups. Moving groups were originally identified by Eggen in the 1950s. However, it has since become clear that many of the older (> 1 Gyr) so called moving groups he identified show a spread in both age and metallicity (Nordstrom et al. 2004), and these kinematic signatures are more likely the result of disk heating by stochastic spiral waves (eg. De Simone, Wu & Tremaine 2004). There is evidence however, that the younger moving groups are coeval. Castro, Porto de Mello & de Silva (1999) found identical Cu and Ba abundances for 7 G and K dwarfs in the Ursa Major moving group, and King et al. (2003) found clear evidence of a correlation between membership of the Ursa Major moving group and activity levels (from CaII H and K emission strength).

Such young moving groups are thought to originate in the same environments as open clusters. Very young clusters should virialise somewhat within their natal gas, and when the gas is cleared by OB star action and the cluster expands, the stars with high enough velocities will become unbound. These unbound stars then slowly expand forming the moving group, and possibly leaving behind an open cluster consisting of any remaining bound stars (see the N-body simulations of Kroupa Aarseth & Hurley 2001). Typical expansion velocities for the unbound population will be $\sim 5\text{--}10 \text{ km s}^{-1}$ ($5\text{--}10 \text{ pc/Myr}$), and the moving group space motion will thus remain quite well defined (superimposed on the more dispersed disk population) until it has had time to become significantly phase mixed by disk heating. Models suggest that phase mixing will increase a moving group velocity dispersion by $\sim 20 \text{ km s}^{-1}$ over ~ 1 Gyr (Asian, Figueras & Torra 1999). Moving groups younger than ~ 1 Gyr should thus consist of young populations with characteristic space motions, and membership of such a group will accurately constrain the age of an eclipsing BD-M dwarf binary just as it would do for open cluster members.

The most notable such groups in the solar neighbourhood are listed in Table 2 along with their kinematic motions and age. Most have open cluster(s) associated with them, which range in size from the rich Pleiades cluster down to the almost evaporated Ursa-Major cluster. In general, each group has one (or two in the case of the Pleiades) distinct kinematic signature. However, note that the Gould belt is rather more complex than the others, since

it consists of an agglomeration of several very young kinematic groups superposed on a less distinct velocity ellipsoid (Moreno, Alfaro & Franco, 1999). Each of the distinct kinematic sub-groups is believed to have a common origin (eg. Asian et al., 1999), with the ellipsoid possibly resulting from an expanding ring of star formation (the local bubble). Interestingly, it appears that a large fraction of young local stars reside in these moving groups. Dehnen (1998) has shown (using Hipparcos astrometry) that the majority of colour selected young disk stars are moving group members, and Makarov (2003) found that a high fraction of X-ray active stars within 50pc belong to the Pleiades and Gould Belt moving groups.

5.3. Identifying young potential moving group members

In order to separate possible young moving group members from the large population of older disk stars, one needs to observationally identify young sources. Age constraints can be placed on young late K and early M dwarfs in a variety of ways. Chromospheric/coronal H_{α} emission from open cluster members (Hawley et al. 1999; Gizis, Reid & Hawley 2002) have shown that there is a well defined, age dependent colour beyond which activity becomes ubiquitous. Despite considerable scatter, all stars redder than this colour are dMe ($EW_{H\alpha} \geq 1.0\text{\AA}$), while the bluer stars are dM without emission. This so called “ H_{α} limit” colour increases with the age of the population, and can identify (in emission) K5-M0 dwarfs younger than $\sim 30\text{Myrs}$, M0-3 dwarfs younger than 100Myrs , and M3-5 dwarfs younger than $\sim 600\text{Myrs}$. Lithium abundances can also provide age constraints. Late K dwarfs deplete lithium over $\sim 100\text{Myrs}$, and early-mid M dwarfs deplete lithium over $\sim 30\text{-}50\text{Myrs}$ (Preibisch et al. 2001; Zapatero-Osorio et al. 2002; Jeffries et al. 2003; Randich et al 2000). One may also constrain ages by fitting isochrones to colour-magnitude data. A $\sim 0.5M_{\odot}$ star will not have fully contracted until it is $\sim 100\text{Myrs}$ old. Therefore, with an accurate parallax distance (possible even at 500pc using the VLT as an interferometer), an appropriate colour-magnitude diagram (see Stauffer et al. 2003), and photometric corrections to account for metallicity sensitive colours (eg. Kotoneva, Flynn & Jimenez 2002), the age of such a star could be approximately constrained.

Clearly, identifying late K and early M dwarfs younger than $\sim 100\text{Myrs}$ will not be difficult. However, older counterparts will be fully contracted, show no lithium and have H_{α} emission $< 1\text{\AA}$. Such sources will require higher resolution analysis if their ages are to be constrained from their activity levels. For instance, one could gauge activity levels by measuring Mg II h & k and Ca II H and K (Doyle et al. 1994; Christian et al 2001; Mathioudakis & Doyle 1991), or by measuring H_{α} at high resolution, and look for weaker line emission in the core of the absorption line (eg. Short & Doyle 1998). These methods

allow one to study activity levels down to those associated with old disk M dwarfs (see Doyle et al. 1994), and should therefore provide an effective way to separate young (<1Gyr) late K and early M dwarfs from older disk stars.

5.4. Kinematic membership of moving groups

Establishing kinematic membership of moving groups will require space motions accurate to a few km s^{-1} . Since accurate radial velocity curves will have been previously measured (to determine BD mass; see Section 4.2), these will provide very accurate centre of mass radial velocities for the binaries. Although it should be possible to derive some proper motions (with the required accuracy) from existing archive measurements (eg. with SuperCOSMOS) sources with distances near 500pc would require some additional effort. Proper motion accuracies would need to be at the milli-arcsecond/year level (cf. $5\text{km s}^{-1} \sim 2\text{mas/yr}$ at 500pc), and it is now quite feasible to measure proper motions of this accuracy using adaptive optics technology with a baseline of $\sim 1\text{-}2$ years (cf. 3mas positional accuracy; Close et al., 2003).

The confidence with which one can assign kinematic membership of a particular moving group will depend on how unique the group's measured kinematic signature is compared to other young moving groups and any non moving group population of young stars (see Figures 1 and 2 of Montes et al. 2001). The Hyades moving group for instance has a space motion well separated from the local standard of rest, but has a rather larger internal dispersion compared to some younger moving groups. As a result some Hyades moving group members will not be obvious kinematic members of the group. At the other extreme, the very young members of the Gould belt and the Pleiades moving group components will not show as much internal dispersion (within each component). However, due to their similar space motions, there is some kinematic overlap between some of these components. Furthermore, young stars that are not members of any moving group can act as a source of potential contamination, if they have the same space motion as the group. However, if the majority of young stars are moving group members (see Section 5.2), such contamination should not be at a high level, and will only decrease membership probabilities by a small amount.

While it is clear that only some fraction of moving group members will be easily identifiable from their kinematics, it is by no means clear exactly what this fraction will be, since there are insufficient radial velocity measurements of young disk stars to properly characterise our expectations. However, it is worth noting that moving group characterisation will certainly improve in the near future, as large scale radial velocity surveys (such as RAVE; Steinmetz 2003) provide radial velocity and metallicity for complete magnitude limited samples.

6. Simulating the number of useful eclipsing BD companions

We will now describe a simulation we have made to predict the size and properties of the population of fully eclipsing BD companions that could be identified by the SuperWASP survey over the whole sky. This simulation predicts how many BDs will be identified, how many of these will be detectable from their secondary eclipse, how many are likely to be significantly irradiated by their primary, and how many will be young (and thus potentially moving group members).

6.1. The simulation

For our simulation, we consider low-mass stars with BD companions in close (~ 0.02 AU) orbits. These binaries will have short orbital periods of 1–1.5d. We thus expect ~ 40 – 60 transits/binary during a ~ 2 month SuperWASP monitoring period, ~ 11 – 16 of which should occur while SuperWASP is taking data (allowing for typical 9h nights and $\sim 25\%$ time lost to bad weather). SuperWASP should experience ~ 9.5 dark nights per lunation, and the moon will be set for typically $\sim 20\%$ of non-dark nights. We therefore expect dark sky conditions $\sim 45\%$ of the time, and would expect ~ 5 – 7 transits to occur during this time. It is therefore appropriate to use the dark sky distance limits for transit detection. We also assumed that for late K dwarfs ($V \sim 16$ near the SuperWASP distance limits) 30% and 75% will be lost due to blending for $b > 20^\circ$ and $b < 20^\circ$ respectively. For the early M dwarfs ($V \sim 18$), $\sim 50\%$ and 85% will be blended for $b > 20^\circ$ and $b < 20^\circ$ respectively (see Section 3.4). We therefore chose to consider only regions of sky with $b > 20^\circ$, and combined this sky coverage with our distance sensitivities to derived space volumes. We then combine these volumes with the nearby luminosity function of Reid Gizis & Hawley (2002) and the vertical disk density law from Zheng et al. (2001), to derived the number of stars within the transit detection limits as a function of M_V . We then factored in a 1% BD companion fraction at a separation of 0.02AU for late K and M dwarfs ($M_V \geq 8$), with a negligible binary fraction for earlier stars (see Section 2.1), and thus determined the fraction of binaries that should be fully eclipsing using the equations from Section 2.2.

In order to factor in how many of these BDs will be detectable from the secondary eclipse, we simulated the BD T_{eff} distribution. This was done by defining an array of ~ 8000 BDs (0.015 – $0.075 M_\odot$) where we assumed a population mass function with $\alpha = 0.5$, and a uniformly distributed random age distribution from 0–10Gyrs. For each BD we then used the NextGen and DUSTY (Chabrier et al. 2000) model isochrones to estimate T_{eff} from mass and age, using linear interpolation between isochrone grid points. We chose NextGen T_{eff} s higher than 2500K, and DUSTY T_{eff} s where the NextGen T_{eff} s were < 2500 K. The

resulting histogram of T_{eff} s is shown in Figure 7. Spectral type ranges (some shown on the figure) were determined using the spectral type – T_{eff} relations from Reid et al. (1999; M6-L2), and Knapp et al. (2004: for $>L2$). For each of our selected spectral type ranges ($M6 \pm 1$ - $T4 \pm 1$) we added up all the BDs in the appropriate T_{eff} range, and divided by the total number, so as to represent the fraction of BDs in that range. These results are tabulated in Figure 7. The implications of this T_{eff} distribution will be discussed in the next section. Finally, we removed any binaries in which the primary was too bright compared to the BD companion (using the M_V limits determined in Section 4.1).

6.2. Simulation results

The simulation predicts that a total of ~ 1000 eclipsing BD companions could be discovered by SuperWASP over the full La Palma sky. Of these, secondary eclipse measurements should allow the BD brightness to be measured (to 10% accuracy) for ~ 150 systems. The predicted distribution of primary and BD spectral types, and BD mass and age for these 150 systems is shown in Figure 8. Note that these predicted results scale with the assumed BD binary fraction and $1/a$, and can thus be easily scaled up or down for different input values. In the top left histogram, the favoured primary spectral types are the earlier types, since these stars are brighter, and detectable out to greater distances. In the top right histogram, there is a strong preference for a BD spectral class of $L4 \pm 1$. This preference results from three factors in our simulation. Firstly, the spectral type– T_{eff} relation we used (Knapp et al. 2004) gives a relatively large T_{eff} range for the L3-5 spectral classes (1500-1900K; see Figure 7). Secondly, L4 companions will be detectable around all the primaries that our simulation considers as potential hosts for BD companions ($M_V > 8$; see Figure 6). Thirdly, although we assume an approximate BD upper mass limit of $0.075M_\odot$, the Dusty models predict a $m_{HBMM} \sim 0.07$. Our simulation thus has the higher mass ($0.07-0.075M_\odot$) objects stabilising their T_{eff} s around 1500-1900K (ie. $L4 \pm 1$) in the 1-10Gyr age range. Uncertainties in the spectral type– T_{eff} relation and the precise value of m_{HBMM} could thus change the spectral type and width of the peak somewhat. However, note that we certainly expect an L4 predominance over later companions, since the L4s are detectable around the brighter primaries. The bottom left histogram shows this preference for $0.070-0.075M_\odot$ objects. Finally, the bottom right histogram shows a strong preference for young BDs, because young BDs are brighter and more easily detectable from their secondary eclipses. The age histogram has ~ 20 binaries younger than 1Gyr, ~ 10 with ages 1-2Gyrs, and a continuum of ~ 2 /Gyr for 2-10Gyrs. This relatively flat age continuum is mainly populated by the $L4 \pm 1$ type companions.

But how many of these detectable BDs would be significantly irradiated? It can be seen by looking at Figure 2 that no BDs with spectral types \leq L0 would be significantly irradiated by any of the primaries we consider. However, an L4 BD would be slightly (\leq 25%) irradiated by the $M_V=8\text{--}9$ primaries. Later BDs would be irradiated by steadily fainter primaries, and the small number of T5 BDs would be irradiated by the majority of primaries. We estimate, using Figure 2 and the top two histograms in Figure 8, that \sim 70% of the predicted companion BDs will not be irradiated by more than 10%.

6.3. A subset of young systems

We also wish to consider the properties of a young subset of the BDs. Such systems are preferred by our detection criteria because BDs are brighter when young. As we discussed in Section 5, many young systems should be members of kinematic moving groups, and as such have ages that can be well constrained. We therefore re-ran our simulation using a T_{eff} distribution derived by only selecting BDs with ages \leq 1Gyr. This simulation predicted \sim 20 binary systems in which BDs could be well measured from the secondary eclipse. The histograms describing these binaries are shown in Figure 9. The primary spectral type histogram is similar in shape to that of the main simulation. The BD spectral type histogram however, is somewhat different to the main simulation. The L4 peak is still there, but has been significantly reduced in number. This is because although the L3–5 T_{eff} range is still relatively large, the majority of the $0.070\text{--}0.075M_{\odot}$ companions (ie. in the 1–10Gyr age range) have been excluded in this age limited simulation. However, there is now an additional peak for M5–9 BDs. This peak results from the fact that all M5–9 dwarfs must be young in order to be BDs, and will thus not be removed by our age constraint. The mass histogram still shows a general preference for higher mass BDs, but the removal of the large number of older $0.070\text{--}0.075M_{\odot}$ objects has decreased the highest mass point significantly. The constrained age histogram is shown with a finer scale, and the preference for younger systems clearly remains. As before, we have used Figure 2 and the top two histograms (this time from Figure 9) to estimate irradiation effects, and estimate that \sim 80% of the predicted young BD companions will not be irradiated by more than 10%. The fraction of the \sim 16 binaries (containing un-irradiated BD companions) that will be clearly associated with a moving group is unclear (see Section 5.4). However, it seems likely that we might expect \sim 10 systems capable of providing BD mass, age, radius, metallicity and luminosity data, for our assumed 1% BD companion fraction.

7. Identification and followup

7.1. Detection rate

On-line optical survey data suggests that we would expect \sim 300,000–1 million sources to $V \sim 18$ in a 320 sq. deg area of sky with $|b| > 20^\circ$ (ie. a typical SuperWASP-I pointing). Typically \sim 70% of these will have $V=16$ –18, and \sim 20% $V=14$ –16. About 20% of sources will be late K and early M dwarfs (\sim 100,000 per 320 sq. degs), with the majority being earlier G and K dwarfs. Of these, \sim 20,000 will be monitored with a sufficient accuracy to detect BD transits (ie. mostly in the $V=14$ –16 range). Typically \sim 30% (\sim 6000) of these are expected to be slightly blended (at the $\geq 1\%$ flux level) with neighbouring sources. We do not expect random fluctuations to produce more than \sim 1 false detection of a 5σ transit event in every \sim 2 million sources (ie. in the full sky late K and M dwarf population). False positives will more likely result from unresolved eclipsing stellar systems in which the eclipsing binary component contributes only a small fraction of the total light. Alonso et al. (2004) report the discovery of 1 transiting planet out of 16 candidates (where the false positives were dominated by such sources).

We might expect \sim 5 genuine fully eclipsing BD companions to be discovered in each \sim 320 sq. deg area of sky (or for instance, 30 per year from SuperWASP-I). Of these, we would expect \sim 15% of binaries (\sim 5 per year) to have measurable (10% accuracy) secondary eclipses, and \sim 1/3 of these to have ages $< 1\text{Gyr}$ (ie. 1–2 per year). These BD detection rates may be scaled for alternative binary criteria – they will scale with BD companion fraction and $1/a$. Note also that the actual transit candidate numbers will be higher, since we have only considered full eclipses, and also expect additional transits by faint low-mass stellar companions, and possibly planetary companions to pass our selection criteria. However, the level at which these will occur is beyond the scope of this paper.

7.2. Followup procedures

The task of identifying eclipsing BD companions will begin with a search of the transit survey database. Automated search algorithms should be used to identify transit signatures in the light curves, allowing for the possibility that there could also be some variation in brightness due to rotationally modulated spot coverage. Large pixels may result in the blending of some sources, so it will be important to confirm the transit source at better spatial resolution. Optical (eg. from the STScI Digitized Sky Survey, or the Super Cosmos Sky Survey) and near infrared (from 2MASS) sky survey images will show if a transit source is a blend of several sources or a single star, and also provide optical/NIR colours and basic

astrometry. These data should also differentiate between dwarfs and giants, confirming or otherwise the faint nature of a transiting companion. It may well also be desirable at this stage to measure additional optical light curve data (using a larger telescope), to both confirm the transit source, and more accurately measure the primary eclipse profile. With the addition of a measured spectral type (and metallicity), the character of the transit will have been well established.

Having confirmed a low luminosity eclipsing companion of a cool dwarf, the next step will be to attempt to measure the secondary eclipse profile and obtain high resolution radial velocity data (see Sections 4.1 and 4.2). A parallax distance to the primary will also be required to confirm its brightness (from which the BD brightness is inferred). Together these data could provide BD mass, radius, metallicity and brightness. The final stage will be to try and determine the age of the system, by measuring accurate astrometry and considering all relevant moving group membership criteria (see Section 5.3).

7.3. Additional issues for young sources

Many young stars may show periodic photometric variability resulting from rotationally modulated spot coverage. This generally occurs at the 5-10% level (Krishnamurthi et al 1998), has periods of \sim 1-5 days (Terndrup et al 2000), and maintains the same modulation shape over numerous rotation periods (Young et al. 1990). The binary systems we consider should produce primary eclipses at least 4% deep, lasting for \sim 1.5hrs, with a period of \sim 1.5d. With such distinct forms of variation, automated search algorithms should be able to identify transit sources even if they show some spot modulation.

Accurately measuring the much fainter secondary eclipses from followup NIR light curves of variable sources could prove more of a challenge. If the primary rotation and BD orbital periods are different, one could simply determine the form of the rotational modulation by phasing the data appropriately, and averaging over several rotation periods. The rotational modulation could then be subtracted off the light curves, leaving only the secondary eclipse dips. However, if the rotation and orbital periods are the same (close binaries can become phase locked by tidal forces; see below), then the eclipse times will always correspond to the same rotational phase.

For a $0.05M_{\odot}$ BD at 0.02AU separation from a primary with mass from 0.6 – $0.35M_{\odot}$ (late K – early M), the spin-orbit synchronisation time-scale varies from \sim 0.04–2.5Gyrs respectively (depending primarily on the primary radius and companion orbital separation; Udry et al. 2002). Such close BD companions around late K dwarfs are thus likely to be

in synchronised orbits, but those around early M dwarfs will probably not have had time to synchronise. To deal with synchronised sources, one could measure simultaneous R-, I- and K-band light curves. The optical bands would contain a negligible fraction of BD flux, and any variability would thus be purely due to rotational modulation. The colour-colour relationship between R-K and R-I modulation away from eclipse could be well determined from the light curve data. This relationship will depend on how the flux in each band changes as spots rotate onto, around and off the observable face of the star. This will of course depend on the temperature, size and surface distribution of spots, but should be a tight relationship for any particular spot configuration. This colour-colour relationship could thus be used to convert R-I measurements (taken during eclipse) into R-K measurements (as if the BD was not eclipsing). The R-band light curve could then be converted into a “pseudo-K-band light curve” (using this R-K colour), which would show only the K-band rotational modulation during eclipse. This could then be subtracted off the original light curve as before. Simultaneous optical/NIR observations would be best done with a robotic telescope with infrared/optical capabilities. The 2-m robotic Liverpool Telescope for example could measure an appropriate set of R- I- and K-band magnitudes in \sim 25 minutes. This would then require light curve coverage of more transits to obtain the required accuracy.

The radial velocity data could also be affected by rotationally modulated spot coverage. As photospheric dark spots and brighter regions rotate over the surface of the star, they can produce radial velocity modulation. These rotational radial velocity variations will have an amplitude up to $v\sin i$, a period equal to the rotation period (P_{rot}), and a oscillatory shape that depends on the distribution of spots across the stellar surface. For illustration, early M stars with ages <100 Myrs fall into three categories of rotation rate. The majority (\sim 60-70%) have slower $v\sin i < 20 \text{ km s}^{-1}$ rotation velocities (with rotation periods of \sim 1-5days). \sim 10-20% are faster rotators ($v\sin i = 30$ -60 km s^{-1}), and only 5-20% are ultra-fast rotators, with $v\sin i > 100 \text{ km s}^{-1}$ (see Mochnacki et al. 2002, and Terndrup et al, 2000, for young field stars and Pleiades stars respectively). The radial velocity oscillation we expect close BD companions to induce is $\sim \pm 20 \text{ km s}^{-1}$, with a period of \sim 1.5days. Clearly in the majority of cases, the rotational velocity modulation will be smaller than the orbital modulation induced by the BD. In general, our task will simply be to deconvolve the two radial velocity components. This should generally be easy. For synchronised orbits, one could measure additional radial velocity data at a later date, when the spot modulation has changed.

8. Conclusions

In order to assess the prospects of discovering eclipsing BD companions capable of yielding mass, age, radius, metallicity and luminosity data, we have assessed what is currently known about such systems. Although close BD companions are fairly rare around late K and early-mid M dwarfs, there could be a $\sim 1\%$ companion fraction at very close ($\sim 0.01\text{--}0.02\text{AU}$) separation. Our knowledge of this companion fraction is poor, but if correct, it suggests that although the BD desert extends into this regime, it is not as dry as for solar type stars.

Using a simulation, and the SuperWASP project as an example, we have predicted the numbers and properties of close BD companions that could be identified by ultra-wide-field transit surveys in the next few years. We assumed a 1% close BD companion fraction at 0.02AU, a uniform age range from 0-10Gyrs, and a BD mass function of $\alpha=0.5$. We estimate SuperWASP to be sensitivite to transits around ~ 1 million late K/early-mid M dwarfs. Based on our current knowledge of BD properties our simulation predicts that ~ 400 BDs in eclipsing binaries could be found. It predicts that ~ 60 of these binaries should have secondary eclipses that are measurable from followup NIR light curves, and should thus provide direct measurement of the BD brightness. The most common detectable BDs are expected to be higher mass BDs orbiting late K-M3 primaries. The majority ($\sim 70\%$) of the detectable BDs should not be irradiated by $>10\%$.

The simulation also reveals a preference for youth amongst binaries containing detectable BDs. This results from the fact that younger BDs are brighter relative to their primary. Our simulation predicts that ~ 20 binaries containing detectable BDs will have ages $< 1\text{Gyr}$. We suggest that it is likely that a significant fraction of such young systems could be young moving group members - disk populations with characteristic space motions that are believed to share a common origin, and thus have an age that can be well constrained (see Section 5). The typical spectral type of the BDs in this young sub-sample ranges from M5–L5, and may be bi-modal, peaking at M5–9 and L3–5. Higher mass BDs are still preferred, but the preference is not as strong for the young subset, and the population is more evenly spread over the mass range $0.040\text{--}0.075M_{\odot}$. We expect $\sim 80\%$ of these young companion BDs not to be irradiated by $>10\%$.

Although some of our input assumptions are rather uncertain, we show that transit surveys such as SuperWASP could find significant numbers of eclipsing BD companions, and by carrying out the followup measurements we describe, it would be possible to accurately determine mass, age, radius, metallicity, and luminosity data for $\sim 10\text{--}20$ young ($< 1\text{Gyr}$ age) BDs. The majority ($\sim 80\%$) of these should not be irradiated above the 10% level, and could thus provide an empirical testbed to compare to theoretical models of free-floating BDs.

We thank Don Pollacco, Francis Keenan, Pete Wheatley, Richard West & Simon Hodgkin for useful discussions. The authors are grateful to PPARC for their support of this work.

REFERENCES

Alonso, R., et al. 2004, *ApJ*, 613, L153

Armitage, P.J. & Bonnell, I.A. 2002, *MNRAS*, 330, L11

Asiain, R., Figueras, F. & Torra, J. 1999, *A&A*, 350, 434

Asiain, R., Figueras, F., Torra, J. & Chen, B. 1999 *A&A*, 341, 427

Bakos, G., Noyes, R.W., Kovács, G., Stanek, K.Z., Sasselov, D.D. & Domsa, I. 2004, *PASP*, 116, 266

Baraffe, I., Chabrier, G., Allard, F. & Hauschildt, P.H. 1998, *A&A*, 337, 403

Benn, C.R. & Ellison, S. 1998, *New Astronomy Reviews*, 42, 503

Bessell, M.S. 1990, *PASP*, 102, 1181

Blundell, J., Jones, H.R.A., Butler, R.P., McCarthy, C., Tinney, C. G., Carter, B.D., Marcy, G.W., Penny, A. J., Pinfield, D. J., 2003, *MNRAS*, submitted

Bouy, H. et al. 2004, *astro-ph/0405111*

Burgasser, A.J., Kirkpatrick, J.D., Reid, I.N., Brown, M.E., Miskey, C.L., Gizis, J.E., 2003, *ApJ*, 586, 512

Burrows, A., Sudarsky, D. & Hubbard, W.B. 2003, *ApJ*, 594, 545

Caldwell, D.A., et al. 2004, *IAUS*, 213, 93

Castro, S., Porto de Mello, G.F. & da Silva, L. 1999, *MNRAS*, 305, 693

Chabrier, G., Baraffe, I., Allard, F. & Hauschildt, P. 2000, *ApJ*, 542, 464

Chabrier, G., Barman, T., Baraffe, I., Allard, F. & Hauschildt, P. H. 2004, *ApJ*, 603, 53

Charbonneau, D., Brown, T.M., Latham, D.W., Mayor, M., 2000, *ApJ*, 529, L45

Christian, D.J., Craig, N., Dupuis, J., Roberts, B.A., & Malina, R.F. 2001, *AJ*, 122, 378

Christian, D.J., et al. 2004, in the proceedings of the Cool Stars 13 conference, ESO SP, in press

Close, L.M., Siegler, N., Freed, M. & Biller, B. 2003, *ApJ*, 587, 407

Dahn, C.C., et al. 2002, *AJ*, 124, 1170

Dehnen, W. 1998, *AJ*, 115, 2384

Delfosse, X., Forveille, T., Mayor, M., Burnet, M. & Perrier, C. 1999, *A&A*, 341, L63

De Simone, R., Wu, X. & Tremaine, S. 2004, *MNRAS*, 350, 627

Dravins, D., Lindegren, L., Mezey, E. & Young, A.T. 1998, *PASP*, 110, 610

Dreizler, S., Rauch, T., Hauschildt, P., Schuh, S.L., Kley, W. & Werner, K. 2002, 391, L17

Els, S.G., Sterzik, M.F., Marchis, F., Pantin, E., Endl, M. & Kurster, M., 2001, *A&A*, 370, L1

Fischer, D.A. & Marcy, G.W. 1992, *ApJ*, 396, 178

Freed, M., Close, L.M. & Siegler, N. 2003, *IAUS*, 211, 261

Gizis, J.E., Kirkpatrick, J.D., Burgasser, A., Reid, I.N., Monet, D.G., Liebert, J. & Wilson, J.C. 2001, *ApJ*, 551, 163

Gizis, J.E., Reid, I.N. & Hawley, S.L. 2002, *AJ*, 123, 3356

Halbwachs, J.L., Arenou, F., Mayor, M., Udry, S. & Queloz, D. 2000, *A&A*, 355, 581

Halbwachs, J.L., Mayor, M., Udry, S. & Arenou, F. 2003, *A&A*, 397, 159

Hawley, S.L., Reid, I.N., & Tourtellot, J.G. 1999, Very Low Mass Stars and Brown Dwarfs, Rebolo, R. & Zapatero-Osorio, M.R., CUP, 109

Hayes, D. S. 1985, Calibration of fundamental stellar quantities, Proceedings of the IAU symposium 111, Dordrecht, D., 225

Henry, G.W., Baliunas, S.L., Donahue, R.A., Fekel, F.C. & Soon, W. 2000, *ApJ*, 531, 415

Henry, T.J. & McCarthy D.J., Jr., 1993, *AJ*, 106, 773

Henry, G., Marcy, G.W., Butler, R.P., Vogt, S.S., 2000, *ApJ*, 529, L41

Henry, T.J., Soderblom, D.R., Donahue, R.A., & Baliunas, S.L. 1996, *AJ*, 111, 439

Horne, K. 2003, Scientific Frontiers in Research on Extrasolar Planets, ASP Conference Series, 294, Deming, D. & Seager, S., 387

Jao, W-C., Henry, T.J., Subasavage, J.P., Bean, J.L., Costa, E., Ianna, P.A., Mendez, R.A., 2003, AJ, 125, 332

Jeffries, R.D., Oliveira, J.M., Barrado y Navascués, D. & Stauffer, J.R. 2003, MNRAS, 343, 1271

Jones, H.R.A., Longmore, A.J., Allard, F. & Hauschildt, P.H. 1996, MNRAS, 280, 77

Kane, S.R., et al. 2004, astro-ph/0406270

Kidger, M.R. & Martín-Luis, F. 2003, AJ, 125, 3311

King, J.R., Villarreal, A.R., Soderblom, D.R., Gulliver, A.F. & Adelman, S. J. 2003, AJ, 125, 1980

Knapp, G.R. et al. 2004, astro-ph/0402451

Konacki, M., Torres, G., Sasselov, D.D. & Jha, S. 2003, ApJ, 597, 1076

Kotoneva, E., Flynn, C. & Jimenez, R. 2002, MNRAS, 335, 1147

Krishnamurthi, A. et al. 1998, ApJ, 493, 914

Kroupa, P., Aarseth, S. & Hurley, J., 2001, MNRAS, 321, 699

Lachaume, R., Dominik, C., Lanz, T., & Habing, H.J. 1999, A&A, 348, 897

Leggett, S.K., Allard, F., Dahn, C., Hauschildt, P.H., Kerr, T.H. & Rayner, J. 2000, ApJ, 535, 965

Leggett S.K. et al. 2002, ApJ, 564, 452

Luhman, K.L. 2004, astro-ph/0407344

Lui, M.C., Fischer, D.A., Graham, J.R., Lloyd, J.P., Marcy, G.W., & Butler, R.P., 2002, ApJ, 571, 519

Lyngå, G. 1987, Catalogue of open cluster data (available through CDS), 5th edition

Makarov, V.V. 2003, AJ, 126, 1996

Makarov, V.V. & Urban, S. 2000, MNRAS, 317, 289

Marchal, L., et al. 2003, Brown Dwarfs, Proceedings of the IAU symposium 211, Martín, E.L., 311

Marcy, G.W. & Benitz, K.J. 1989, *ApJ*, 344, 441

Mathioudakis, M. & Doyle, J.G. 1991, *A&A*, 244, 409

McCaughrean, M.J. et al. 2004, *A&A*, 413, 1029

Mochnacki, S.W., et al. 2002, *AJ*, 124, 2868

Montes, D., López-Santiago, J., Gálvez, M.C., Fernandez-Figueroa, M.J., De Castro, E. & Cornide, M., 2001, *MNRAS*, 328, 45

Moreno, E., Alfaro, E.J. & Franco, J. 1999, *ApJ*, 522, 276

Mountain, C.M., Leggett, S.K., Selby, M.J., Zadrozny, A. 1985, *A&A*150, 281

Nidever, D.L., Marcy, G.W., Butler, R. P., Fischer, D. A. & Vogt, S. S. 2002, *ApJS*, 141, 503

Nordström, B. et al., 2004, *A&A*, 418, 989

Odenkirchen, M., Soubiran, C. & Colin, J. 1998, *New A*, 3, 583

Oppenheimer, B.R. et al., 2001, *AJ*, 121, 2189

Pickles, A.J. 1985, *ApJS*, 59, 33

Pinfield, D.J., Dobbie, P.D., Jameson, R.F., Steele, I.A., Jones, H.R.A., Katsiyannis, A.C., 2003, *MNRAS*, 342, 1241

Preibisch, T., Guenther, E. & Zinnecker, H. 2001, *AJ*, 121, 1040

Randich, S., Pasquini, L. & Pallavicini, R. 2000, *A&A*, 356, L25

Reid, I.N. & Cruz, K.L. 2002, *AJ*, 123, 2806

Reid, I.N., Gizis, J.E. & Hawley, S.L. 2002, *AJ*, 124, 2721

Reid, I.N., Gizis, J.E. Kirkpatrick, J.D., Koerner, D.W., 2001, *AJ*, 121, 489

Reid I.N., et al. 1999, *ApJ*, 521, 613

Reid, I.N. & Mahoney, S. 2000, *MNRAS*, 316, 827

Reiners, A., 2004, in Proceedings of the 13th Cool Stars Workshop, ESA Special Publications series, in press

Reipurth, B. & Clarke, C. 2001, AJ, 122, 432

Ribas, I. 2003, A&A, 400, 297

Santos, N.C., et al., 2002, A&A, 392, 215

Sarajedini, A., von Hippel, T., Kozhurina-Platais, V., & Demarque, P. 1999, AJ, 118, 2894

Schuh, S.L., et al. 2003, A&A, 410, 649

Short, C.I. & Doyle, J.G. 1998, A&A, 336, 613

Soderblom, D.R., Duncan, D.K., & Johnson, D.R.H. 1991, ApJ, 375, 722

Soderblom, D.R. & Mayor, M. 1993, AJ, 105, 226

Song, I., Zuckerman, B. & Bessell, M.S. 2003, ApJ, 599

Stauffer, J.R. et al. 2003, AJ, 126, 833

Stauffer, J.R., Schultz, G. & Kirkpatrick, J.D., 1998, ApJ, 499, 199

Steinmetz, M. 2003, GAIA Spectroscopy: Science and Technology, ASP Conference Proceedings, Munari, U., 298, 381

Terndrup, D.M. et al., 2000, AJ, 119, 1303

Udalski, A., et al. 2002a, Acta Astron., 52, 1

Udalski, A., et al. 2002b, Acta Astron., 52, 115

Udalski, A., et al. 2003, Acta Astron., 53, 133

Udry, S., Mayor, M., Naef, D., Pepe, F., Queloz, D., Santos, N.C., Burnet, M., 2002, A&A, 390, 267

Vogt, S.S., Butler, R.P., Marcy, G.W., Fischer, D.A., Pourbaix, D., Apps, K. & Laughlin, G., 2002, ApJ, 568, 352

Wilson, J.C., Kirkpatrick J.D., Gizis, J.E., Skrutskie, M.F., Monet, D.G. & Houck, J.R., 2001, AJ, 122, 1989

Young, A., Skumanich, A., MacGregor, K.B. & Temple, S. 1990, ApJ, 349, 608

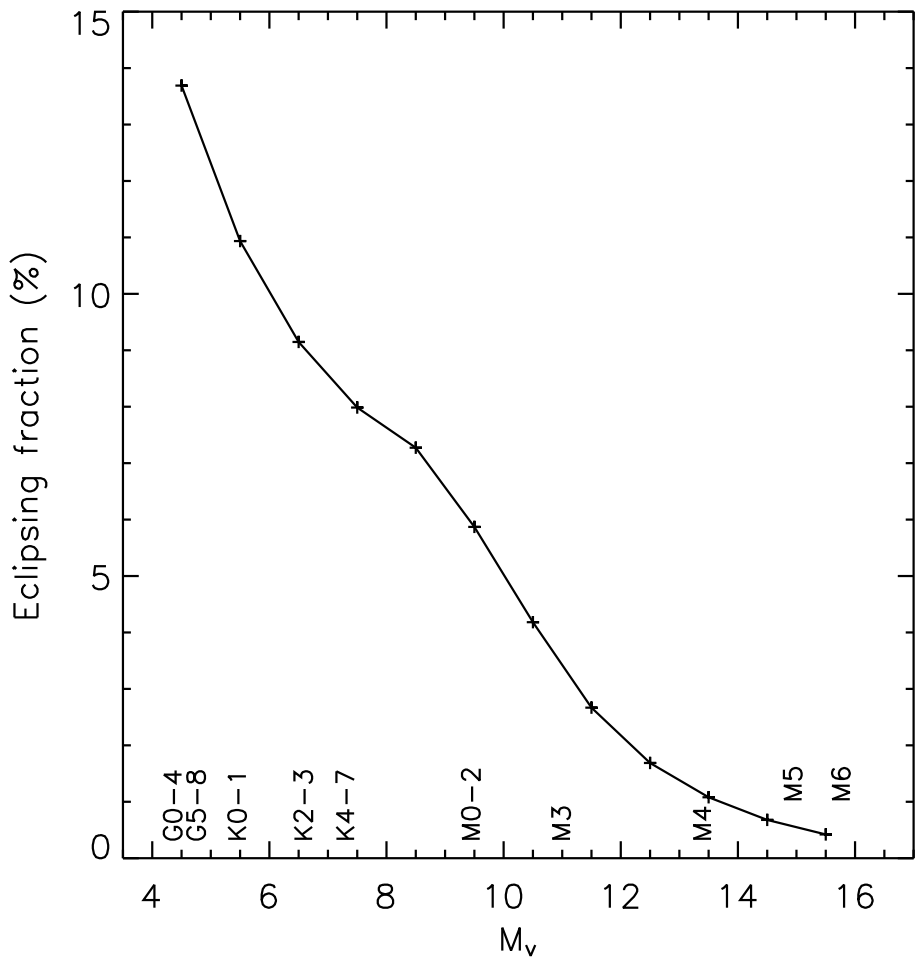


Fig. 1.— The fraction of companion BDs ($0.1R_\odot$) that will fully eclipse their primary star at a separation of 0.02AU, against primary type.

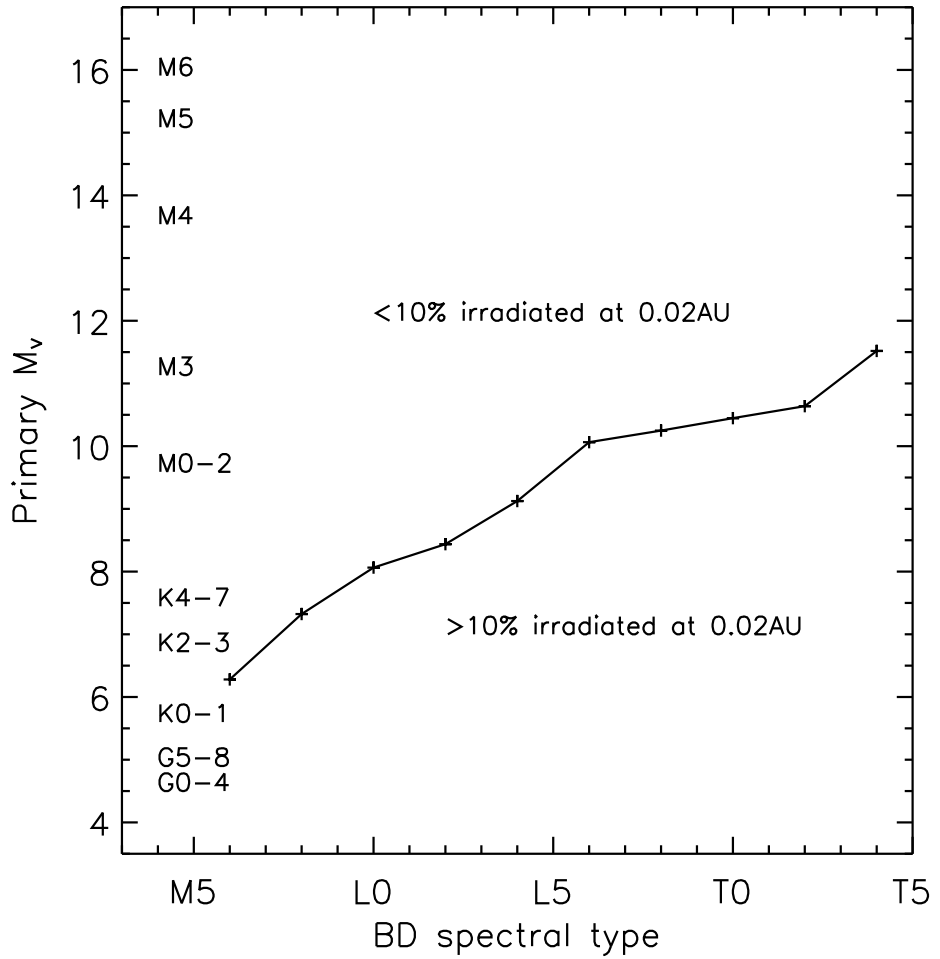


Fig. 2.— Primary M_V against the companion BD spectral type. The solid line represents binary systems in which the BDs are irradiated by 10% at a separation of 0.02AU. The regions above and below the line represent lower and higher levels of BD irradiation respectively.

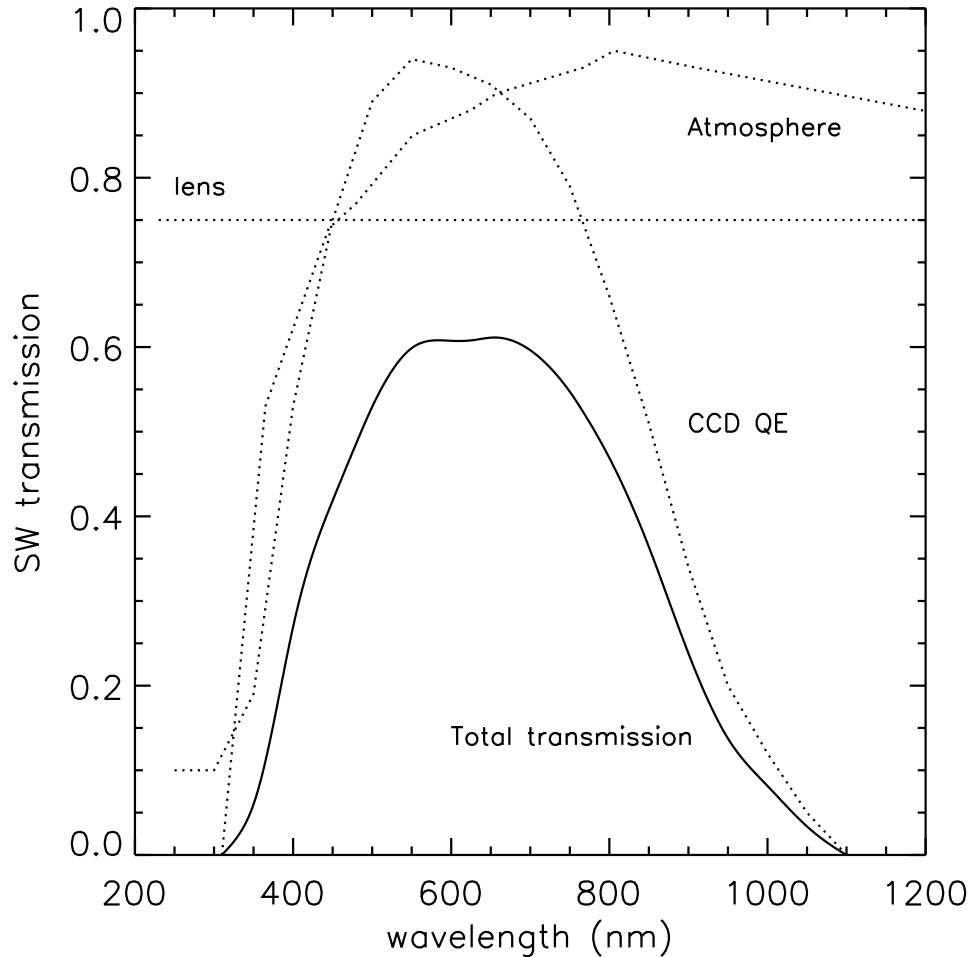


Fig. 3.— The transmission of SuperWASP. Atmospheric transmission (airmass=1.5), optical throughput and CCD quantum efficiency are shown with dotted lines. The total transmission is shown with a solid line.

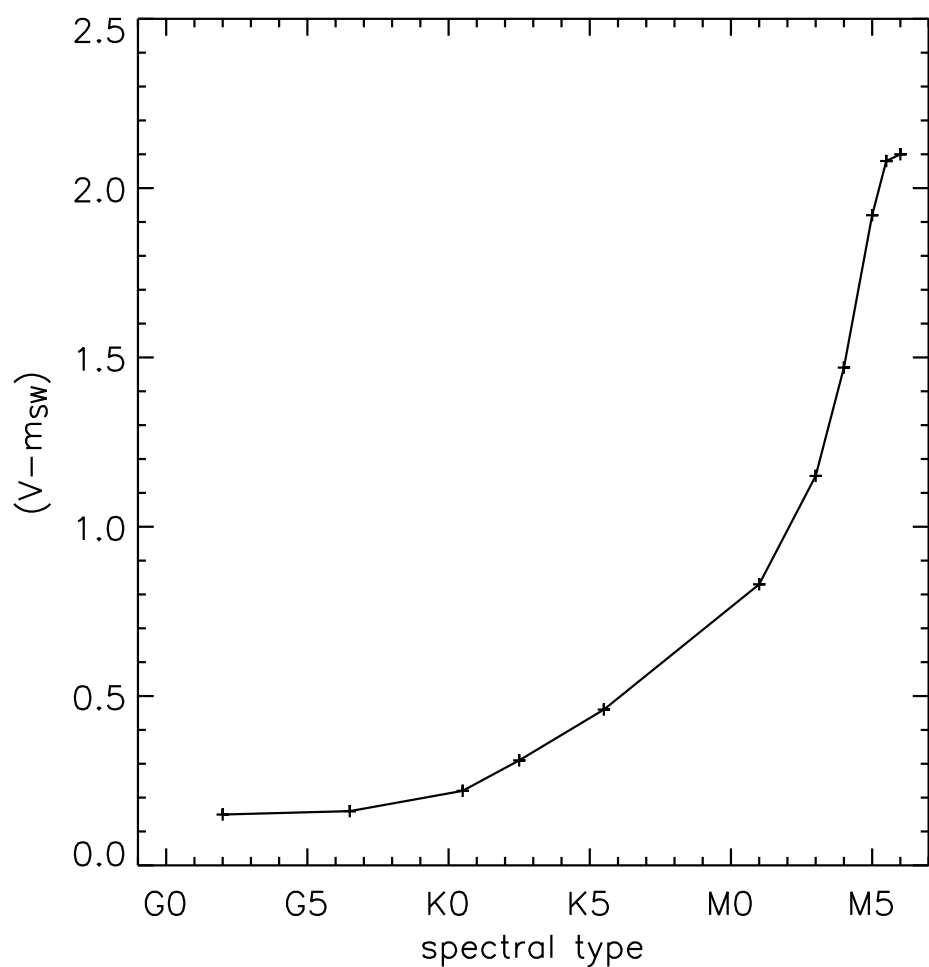


Fig. 4.— Synthetic $(V - m_{SW})$ colour against dwarf spectral type.

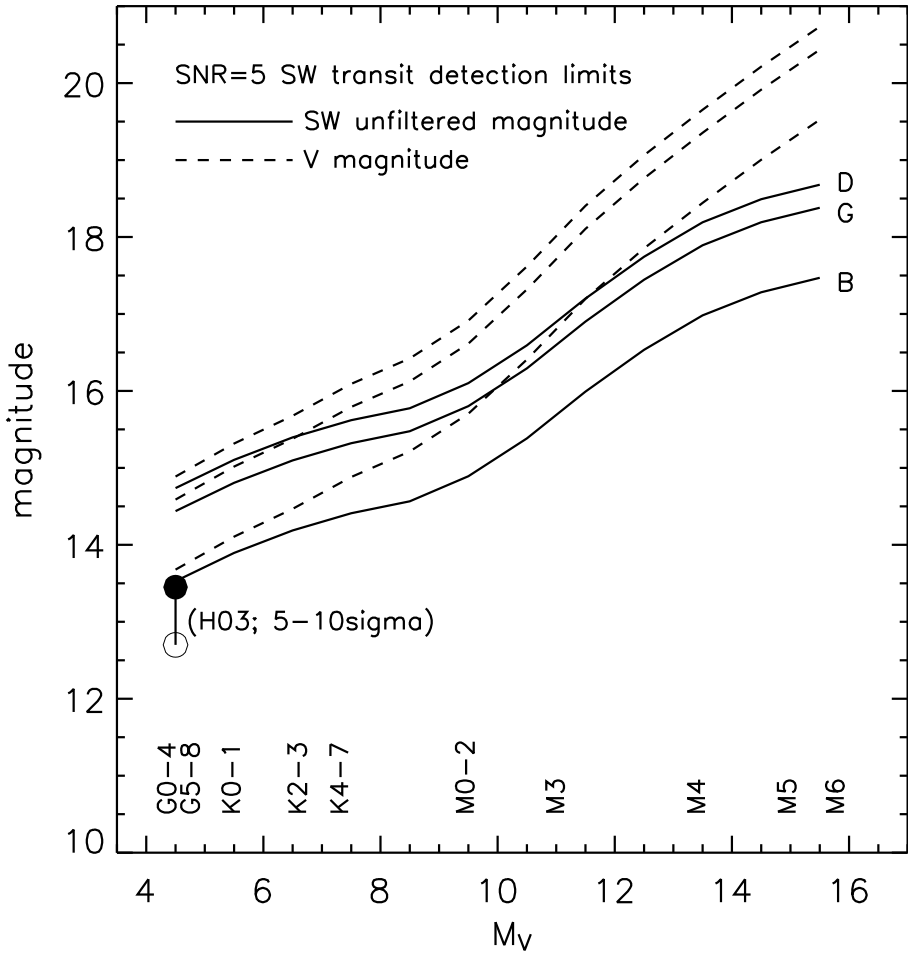


Fig. 5.— SuperWASP magnitude limits for 5- σ BD ($0.1R_{\odot}$) transit detections against primary type. Limits are shown for dark (D), grey (G) and bright (B) skies. Solid lines show magnitudes in the SuperWASP system. Dashed lines signify the SuperWASP limits converted into V magnitudes. A point from Horne (2003) is shown for comparison.

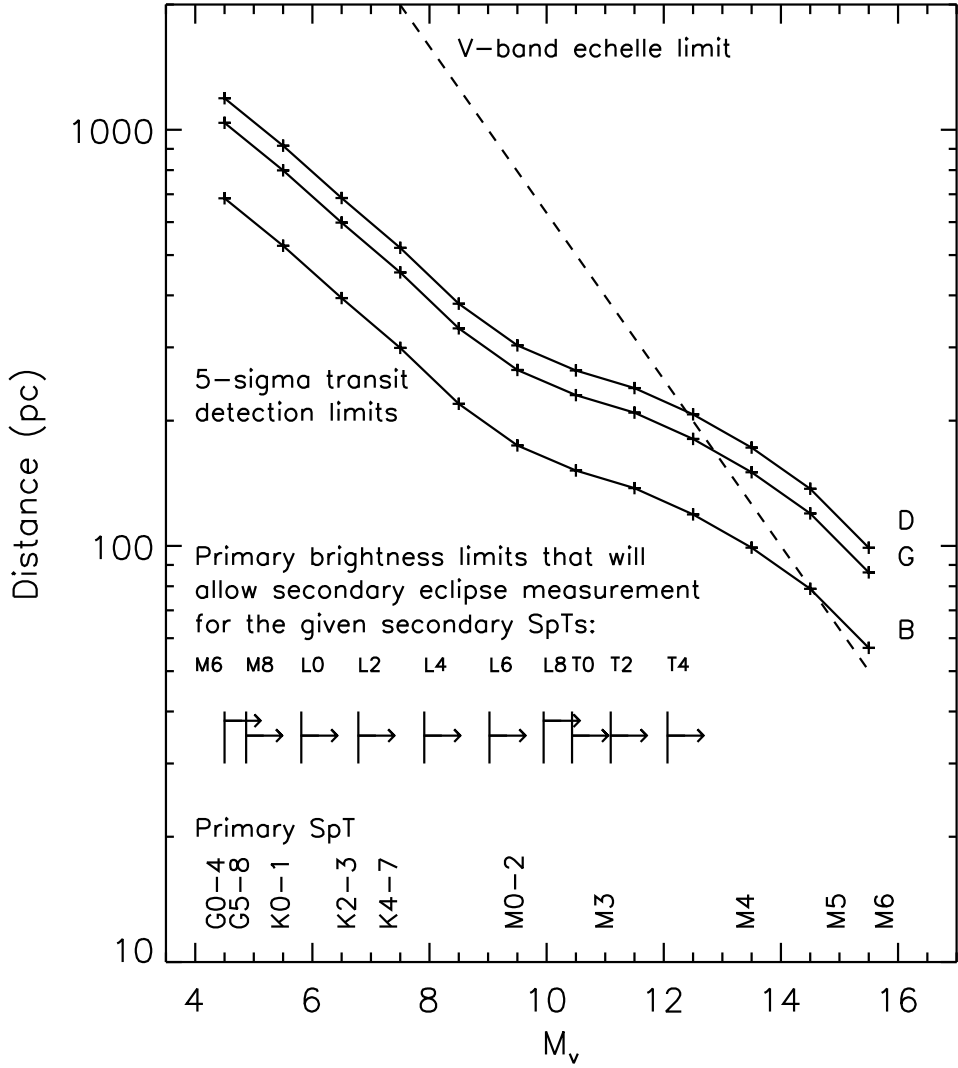


Fig. 6.— Detection and follow-up limits for transiting BD companions. The solid lines show the distance limits for 5σ BD transit detections (for dark, grey and bright skies) against primary type. The dashed lines indicate distances out to which the mass of a $0.05M_{\odot}$ BD at 0.02AU separation could be accurately measured with V- and I-band echelle spectroscopy on an 8-m telescope. The M_V lower limits shown indicate the maximum brightness a primary star may have if we are to be able to measure the brightness of a BD companion (with spectral type of T4-M6) with 10% accuracy, from a near infrared light curve of the secondary eclipse.

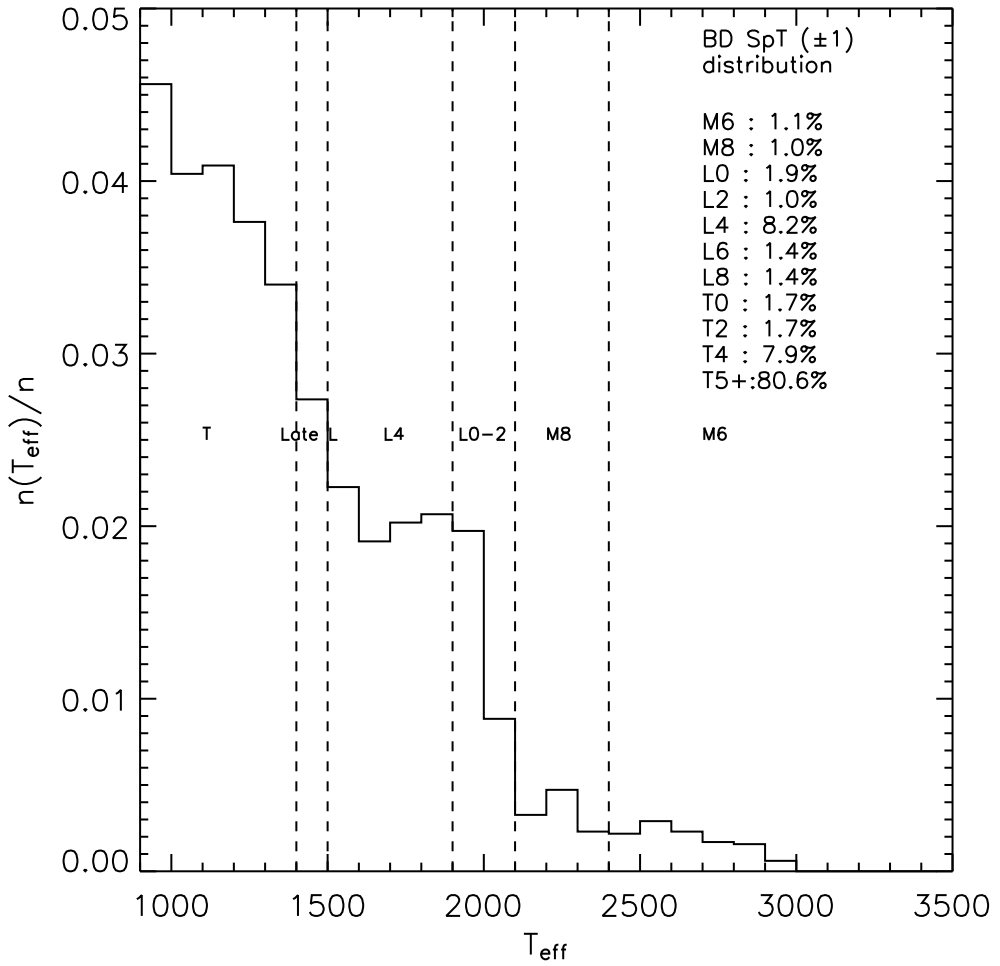


Fig. 7.— The T_{eff} distribution for a population of BDs with a uniform age spread from 0-10Gyrs, and an $\alpha=0.5$ mass function. Some spectral type divisions are indicated with dashed lines. The fraction of BDs in spectral type ranges from M6-T4 is given in the top right of the plot. Note that many BDs are cooler than 900K, although the plot does not cover this T_{eff} range.

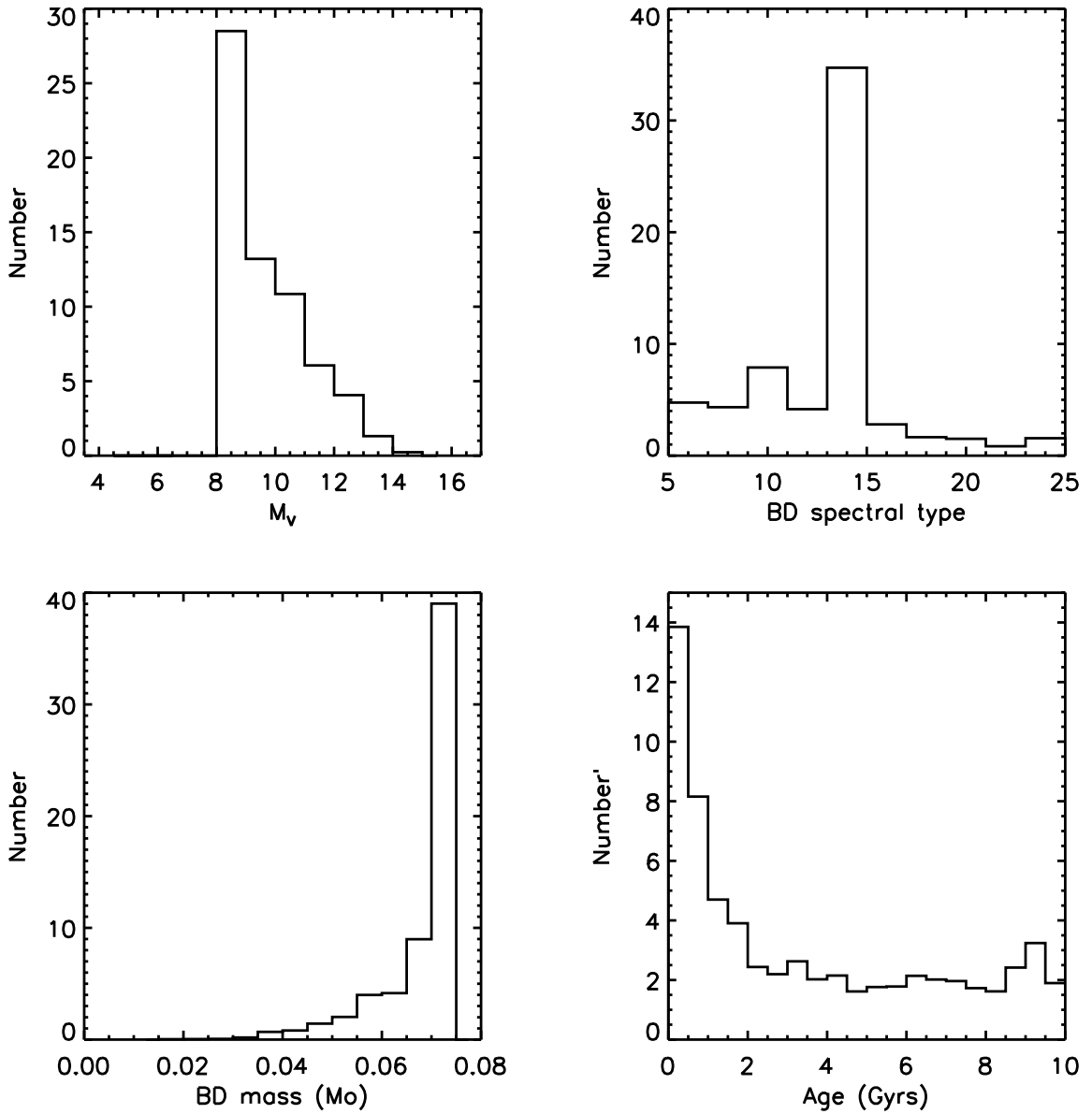


Fig. 8.— Predicted numbers of fully eclipsing brown dwarf companions with measurable secondary eclipses, that could be found by SuperWASP. The four sub-panels show the primary and BD spectral type distributions, and the BD mass and age distributions.

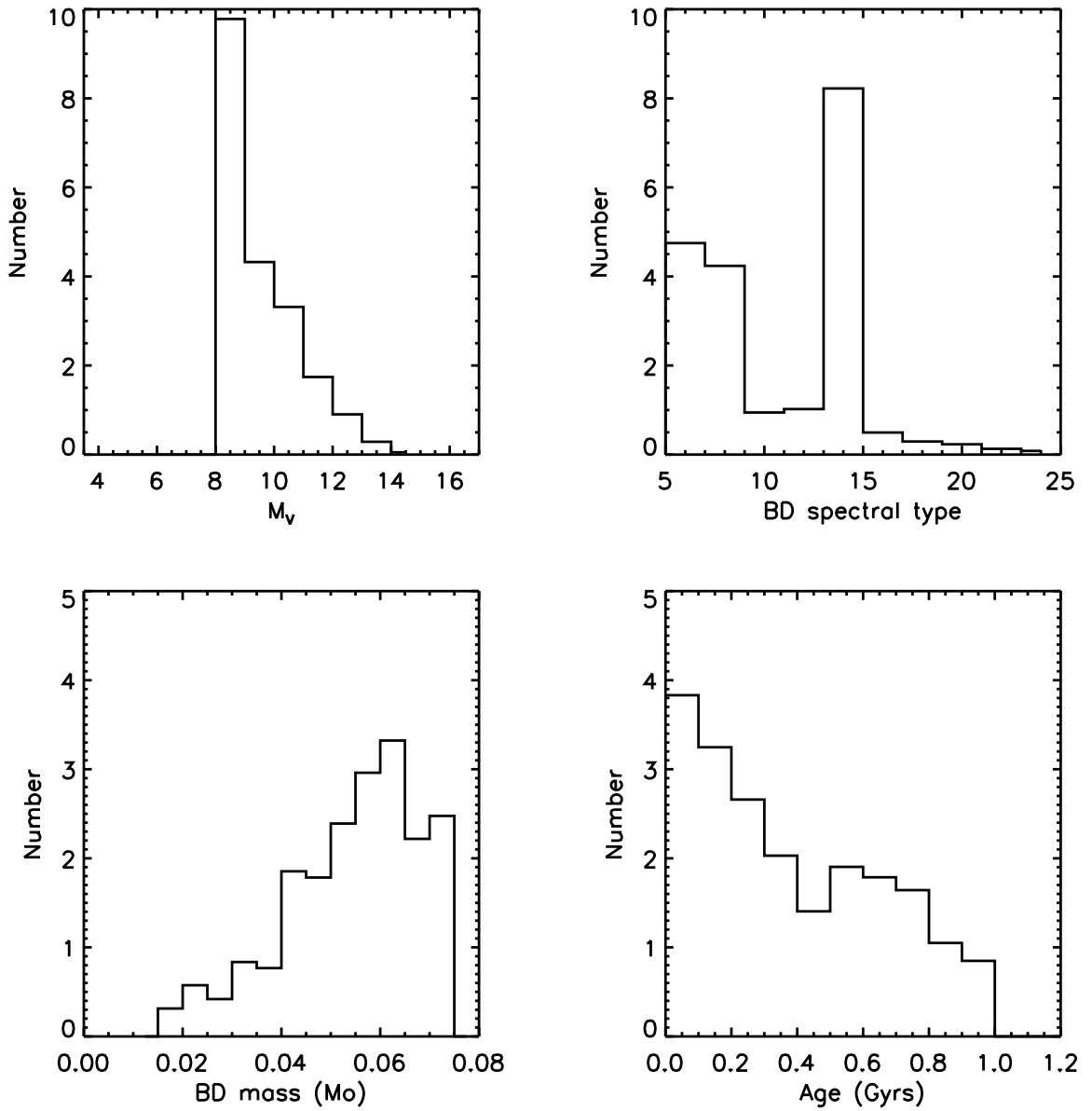


Fig. 9.— The same as figure 8, but for systems with ages <1Gyr.

Table 1: Brown dwarf companion fractions as a function of primary type. Companion fractions have been estimated from the following; (1) Halbwachs et al. (2000); (2) Duquennoy & Mayor (1991); (3) Vogt et al. (2002); (4) Blundell et al. (2004); (5) Els et al. (2001); (6) Lui et al. (2002); (7) Gizis et al. (2000); (8) Wilson et al. (2001); (9) Reid & Mahoney (2000); (10) Marchal (2003); (11) Nidever et al. (2003); (12) Oppenheimer et al. (2001); (13) Reiners (2004); (14) Pinfield et al. (2003); (15) Burgasser et al. (2003); (16) Close et al. (2001); (17) Reid et al. (2001).

| Stellar companions | | | | | | | |
|--|-----------------------------|-------------------------------|------------|------------------------|--|----------------------|-----------------------------|
| Separation (AU) | 0.001–0.01 | 0.01–0.1 | 0.1–1 | 1–10 | 10–100 | 100–1000 | 1000–10000 |
| F, G & K primaries ($R_{\odot}=0.005\text{AU}$) | – | $\sim 4\%$ per decade (1) | | | $\sim 10\text{--}15\%$ per decade (2) | | |
| Brown dwarf companions | | | | | | | |
| Separation (AU) | 0.001–0.01 | 0.01–0.1 | 0.1–1 | 1–10 | 10–100 | 100–1000 | 1000–10000 |
| F, G & K ($R_{\odot}=0.005\text{AU}$) | – | $<0.07\%$ per decade (3,4) | | | ? | $\sim 10\%$ (5,6) | $5\text{ -- }13\%$ (7,8) |
| Early – mid M | $0\text{ -- }2\%$ (9,10) | ? | 1% (11) | 1% (11) | 1 – 3% (12) | – | – |
| late M, L & T | $\leq 30\%$ (13,14) | | | 10 – 20% (15,16,17) | – | – | – |

Table 2: Summary of the kinematic moving groups that make up the local young disk population.

| Moving group (comments, refs) | U, V, W (km s^{-1}) | Age (Myrs) | Includes |
|---|-----------------------------------|--------------------|--|
| IC 2391 (1) | -21, -16, -9 | 35-55 | IC 2391 cluster |
| Gould Belt Velocity ellipsoid with some substructure (some structures sometimes associated with the Pleiades MG) (2, 3, 4) | U~V~W ~20-0 | 10-90 | Sco-Cen, Cas-Tau Carina-Vela and TW Hydra assocs |
| Pleiades (aka Local association. Contains two main velocity substructures) (5, 6) | -9, -26, -9 -17, -22, -6 | 100-150 200-300 | Pleiades, Alpha Per, and NGC 2516 clusters M34 cluster |
| Castor (7) | -11, -8, -10 | ~320 | The A-stars Vega and Fomalhault |
| Coma Berenices (8) | -10, -5, -8 | 250-400 | Coma Ber cluster (aka Melotte 111) |
| Ursa Major (aka Sirius super-cluster) (9) | +15, +1, -11 | 400-600 | Ursa Major cluster |

Table 2: Continued.

| | | | |
|--|---------------|------|------------------------------|
| NGC 1901 (10) | -25, -10, -15 | ~500 | NGC 1901 cluster |
| Hyades (11) | -40, -18, -2 | ~600 | Hyades and Praesepe clusters |
| <i>References</i> | | | |
| 1. Lynga (1987) 2. Moreno, Alfaro & Franco (1999) 3. Makarov & Urban (2000) 4. Song, Zuckerman & Bessell (2003) 5. Asiain, Figueras & Torra (1999) 6. Asiain, Figueras, Torra & Chen (1999) 7. Ribas (2003) 8. Odenkirchen, Soubiran & Colin (1998) 9. King et al., 2003 10. Dehnen (1998) 11. Montes et al., (2001) | | | |